Hindawi Publishing Corporation
Journal of Nanomaterials
Volume 2016, Article ID 8563870, 8 pages
http://dx.doi.org/10.1155/2016/8563870

Research Article

Stable Dispersed MoS_2 Nanosheets in Liquid Lubricant with Enhanced Rate of Penetration for Directional Well

Fuwei Lu,[1] Hui Du,[2] Zhaojun Chen,[2] Xianbin Zhang,[3] Houping Gong,[1] and Yun Xue[4]

[1]*Sinopec Huadong Oil Engineering Co., Ltd., Yangzhou 225009, China*
[2]*College of Chemistry and Chemical Engineering, Qingdao University, Qingdao 266071, China*
[3]*CNPC Bohai Drilling Engineering Co., Ltd., Tianjin 300280, China*
[4]*Sinopec Engineering Technology Institute of Jiangsu Oilfield Company, Yangzhou 225009, China*

Correspondence should be addressed to Fuwei Lu; lufuwei@hotmail.com and Hui Du; duhuiqdu@163.com

Received 2 August 2016; Accepted 25 September 2016

Academic Editor: Simo-Pekka Hannula

MoS_2 nanosheets of approx. 100 nm were synthesized by a reverse microemulsion route firstly, then were annealed under nitrogen atmosphere, and were finally modified with 1-dodecanethiol. The prepared MoS_2 nanosheets were characterized by XRD, TEM, FTIR, and so forth. Experimental results show that MoS_2 nanosheets with the typical layer structure can be easily dispersed in oil lubricant for rate of penetration (ROP) increasing in directional well. The ROP of directional well with the prepared liquid lubricant was 52.9% higher than that of the similar directional wells at least, and the drilling velocity was increased 20% while the total proportion of lubricant in drilling fluid was 1.5%.

1. Introduction

The contradiction between lubrication and drilling complications downhole became an increasingly prominent problem, while the number of extended reach wells, slim hole wells, ultra-deep wells, and other complex structures increased [1]. Currently, the using of environment friendly lubricants such as vegetable oils [2–4], emulsified wax [5], and so forth could not handle soft mudstone, fluid stone (shale), and other downhole difficulties effectively in large angle gradient or horizontal wells.

With consideration to eliminating drilling problems such as low rates-of-penetration (ROP), wellbore stability, poor hole cleaning, and stuck pipe, a new type of lubricant with bonding capability has been developed. Fatty acid ammonium was synthesized by Xiang and Amin from Baker Hughes, which was then blended with fatty acid methyl ester to form a new lubricant [6]. The fatty acid ammonium was prone to be adsorbed onto drilling instruments and rock surface, thereby enhancing lubrication and the ability to stabilize the wall. In 2011, Navarro et al. from EGS Universal Ltd. introduced a bonding drilling fluid lubricant named DFL [7]. The active ingredient of DFL can produce a smooth surface by free ions within the wellbore association, which can control the vortex flow interface effectively. Using DFL can reduce frictional force and improve ROP in building-up section of extended reach wells and so forth. It can also improve the timeliness 50% even at large borehole curvature while the proportion of lubricant in drilling fluid is 3~6%.

Although the bond-type lubricants show superior properties to conventional lubricants, those are still liquid lubricants. Only limited lubrication is obtained under extreme conditions, which cannot provide sufficient strength to reduce friction and protect drilling tools. According to research reports, under a single thrust bearing tester the nanosolid's coefficient of friction is less than that of pure oil while the extreme pressure of the nanolubricant is two times higher than that of pure oil [8–11]. In order to improve ROP and protect the drilling tool under high angle downhole, boron-based nanolubricant was introduced in liquid lubricant by Krishnan et al. [12] The boron-based nanolubricant showed a remarkable improvement of ROP by the crystallized layers of boron nanoparticles, which meant that the crystallized solid layers could provide effective lubrication in directional well. On the other hand, MoS_2 nanoparticles make a hard, brittle material that is cheap and

readily available on the market, but it was seldom reported in drilling fields. MoS_2 is a typical two-dimensional layered material and has been widely used for lubrication [13–15]. Many studies have reported on a friction reduction and a prolonged life expectancy when MoS_2 fillers are dispersed in oils [16–18]. However, the lubrication performance of solid MoS_2 was always limited by the poor disperse state in oil phase. In order to improve the steady-state wear behavior and lubrication performance, the solid MoS_2 was combined with other mediums, such as ionic liquids and polymers [19, 20]. If the solid MoS_2 was coupled with organic chains, the steady-state wear behavior and lubrication properties of MoS_2 in liquid oils might be much better.

To increase ROP in directional well, MoS_2 was synthesized and modified with 1-dodecanethiol and then blended into liquid lubricant. The dispersion state of the modified MoS_2 in liquid lubricant was mentioned in this paper. The lubricating property was also evaluated and the effect of the lubricant on the performance of drilling fluid was tested. The ROP data of evaluation well was collected and analyzed by using the liquid lubricant with MoS_2 nanosheets additive.

2. Materials and Methods

2.1. Preparation and Characterization of MoS_2 Nanosheets. All the chemicals were purchased from Sinopharm Chemical Reagent Co. Ltd. and were analytically pure and used as received. The MoS_2 nanosheets were prepared in a Triton X-100/1-hexanol/cyclohexane/water reverse microemulsion. In a typical preparation process, 7.2 parts (mass ratio) of Triton X-100, 4.8 parts of 1-hexanol, and 8.0 parts of cyclohexane were mixed with 6.0 parts of $(NH_4)_2MoS_4$ aqueous solution (0.1 M) or hydroxylamine hydrochloride/HCl aqueous solution (0.3 M/1.0 M) at 50°C by magnetic stirring to prepare Mo precursor reverse microemulsion and reductant reverse microemulsion, respectively. After that, the reductant reverse microemulsion was dropwise added in Mo precursor reverse microemulsion and then reacted for 4 h at 50°C with continuous magnetic stirring. Then the mixed reverse microemulsions were placed and aged for 2 days. The obtained dark brown precipitate (denoted as RM-MoS_2) was collected by centrifugation, washed with water/ethanol mixed solution 6 times, and dried at 50°C in a vacuum oven. RM-MoS_2 was annealed at 800°C under nitrogen atmosphere for 2 h to improve the crystallinity. Then the annealed products were modified with 1-dodecanethiol (DDT) as follows: 0.5 parts of the annealed products and 10 parts of 1-dodecanethiol were dispersed in 30 parts of methanol by ultrasonic processing for 30 min; then the suspension was heated at 45°C with magnetic stirring for 6 h; the modified products (denoted as DDT-MoS_2) were collected, washed, and dried at 50°C for 8 h in a vacuum oven.

The crystal structure of the MoS_2 products was determined by X-ray diffraction (XRD) using a PANalyitcal X'Pert PRO MPD X-ray diffractometer with Cu Kα radiation (λ = 0.15418 nm) with 2θ ranging from 10° to 70°. A Nicolet Magna-750 Fourier Transform Infrared (FTIR) spectrometer was used to record the FTIR spectra of MoS_2 products. The morphology and size of the MoS_2 in liquid lubricant were measured by using a JEOL JEM-2100F transmission electron microscope.

2.2. Preparation and Tests of Liquid Lubricant. The lubricant JS-LUB was prepared using the following compositions: base olefin, vegetable oil, vegetable oil acids, amine, polysiloxane, and DDT-MoS_2. DDT-MoS_2 was first dispersed in base olefin. The blending conditions were listed as follows: temperature is 50°C and stirring rate is 800 rpm. The proportion of DDT-MoS_2 in JS-LUB was about 0.4~0.8 wt%. The dispersed DDT-MoS_2 in base olefin was then mixed in other constituents. No emulsifiers were added. The dispersion state of DDT-MoS_2 and RM-MoS_2 in base olefin was observed after 24 hours without interference.

KD-21C and KD-51 used in the adjoining wells were purchased from Yangzhou Runda Oilfield Chemicals Co., Ltd. KD-21C was composed of base olefin, vegetable oil, vegetable oil acids, amine, and emulsifiers. The major components of KD-51 were base olefin, polyolefin, water, and emulsifiers. The aqueous phase of drilling fluid and the lubricant oil droplets was kept stable by the emulsifiers used in KD-21C and KD-51.

The lubricants were typically mixed into a 1.03 g/cm^{-3} lab-prepared base drilling fluid. The concentration of lubricant in base drilling fluid is equivalent to 0.26% lubricant (w/w) or to 0.5% lubricant (w/w), assuming a nominal density of 0.8 g/cm^{-3} for the lubricant. After adding the lubricants to the base drilling fluid, coefficient of rubbing (C_f) measurements for each sample was obtained with an Ofite 112 EP Lubricity Meter. The test consisted of measuring the torque on a steel block that is being pressed against a rotating steel ring. Tests were conducted at room temperature with a speed of 60 rpm and 150 inch-lbs of torque contact. The rheological behavior of drilling fluids was studied by rotatory viscometer and fitting by Bingham model. Evaluation endpoints include plastic viscosity (PV), yield point (YP), and ratio of yield stress to plastic viscosity (YP/PV). The data of API filter loss (FL_{API}) and density of drilling fluid were also collected.

3. Results and Discussion

3.1. Characterization of MoS_2. XRD patterns of the MoS_2 products are shown in Figure 1. No diffraction peaks are observed in Figure 1(a), indicating that RM-MoS_2 prepared in reverse microemulsion system is amorphous. After annealing and modification processes, the crystallinity of MoS_2 products is significantly improved that all X-ray diffraction peaks of DDT-MoS_2 (Figure 1(b)) can be indexed to the hexagonal 2H MoS_2 (JCPDS 37-1492, Figure 1(c)) [21].

The morphology, size, and crystal structure of the MoS_2 in JS-LUB were observed by transmission electron microscope (TEM) and high-resolution TEM (HRTEM). As shown in Figures 2(a) and 2(b), the RM-MoS_2 samples are irregularly shaped amorphous flakes with mean size of 100 nm, which is consistent with the XRD result. During the annealing process, the small RM-MoS_2 flakes agglomerated, and the crystal structure was transformed to characteristic two-dimensional layered structure from amorphous state (Figures 2(c) and 2(d)). The distance of the two layers was about 0.64 nm.

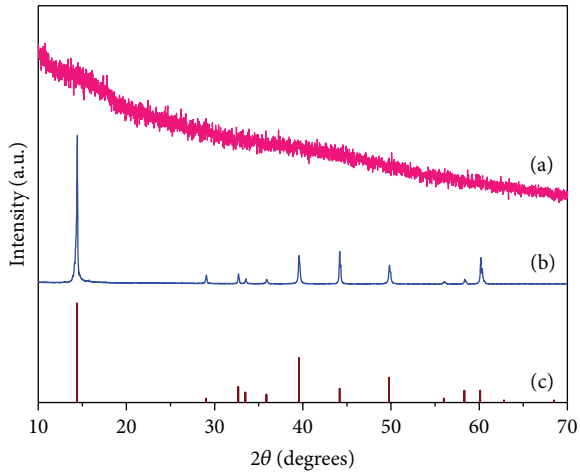

Figure 1: XRD patterns of (a) RM-MoS_2, (b) DDT-MoS_2, and (c) JCPDS 37-1492.

The dispersion state of RM-MoS_2 and DDT-MoS_2 in base olefin after 24 h is shown in Figure 3. As can be seen from Figure 3, most of the RM-MoS_2 particles are deposited on the bottom of the bottle. After being modified with 1-dodecanethiol, the surface of MoS_2 was adsorbed with C12 organic chains, which has shown good compatibility with the base olefin. The DDT-MoS_2 particles are dispersed in base olefin without deposits.

FTIR spectra of RM-MoS_2 and DDT-MoS_2 were determined to verify the adsorption situation on the surface of as-synthesized MoS_2 and JS-LUB. As shown in Figure 4, three intense absorption bands at 1460 cm^{-1} and 2960–2850 cm^{-1} are shown in the FTIR spectra of both RM-MoS_2 and DDT-MoS_2, which would be identified as the characteristic absorption of C-H and indicate the absorption of Triton X-100 or DDT on the MoS_2 nanoflake surface [22]. The FTIR spectrum of RM-MoS_2 (Figure 4(c)) shows absorption bands of aromatic ring at 1600 cm^{-1} and 1501 cm^{-1}, as well as the absorption band of ether band (C-O-C) at 1124 cm^{-1}, which confirm the absorption of Triton X-100 on RM-MoS_2 surface. Besides, the broadband at 3300–3500 cm^{-1} should be assigned to the adsorbed H_2O. In the FTIR spectrum of DDT-MoS_2 (Figure 4(b)), all the above characteristic bands of aromatic ring and ether band disappear, which indicate the vanishing of Triton X-100 during annealing process and the new adsorption of DDT on MoS_2 nanoflake surface. In the FTIR spectra of JS-LUB, in addition to the absorption bands of DDT-MoS_2, the intense absorption band at 1739 cm^{-1} should be assigned to the stretching vibration of C=O in vegetable oil acids [23], the weak absorption band at 1165 cm^{-1} should be assigned to the bending vibration of C=C, and the weak absorption bands at 1075 cm^{-1} and 1021 cm^{-1} should be assigned to the bending vibration of C-Si [24].

3.2. Lubricity Properties. The properties and lubricity of JS-LUB and two commercial lubricants are shown in Table 1. As can be seen from Table 1, the lubricating decrease rate of base oil is only 7.8%, even though the oil phase is the main active component of the lubricant. This is because the base oil cannot be effectively dispersed in the aqueous phase of the drilling fluid; only a small part reaches the rubbing surface requiring lubrication. The oil phase of KD-21C and KD-51 can be dispersed into small particles of oil droplets by emulsifiers, which can be dispersed in the aqueous phase uniformly. The oil droplets can reach the rubbing surface much easier with the aqueous phase and act as the lubricating medium. Lower rates of C_f were over 85% in base drilling fluid of both KD-21C and KD-51. The action principle of JS-LUB was quite different from KD-21C and KD-51. The organic acid ammonium in JS-LUB can be effectively absorbed on the rubbing surface, which acts as the bridging between the rubbing surface and vegetable oil, base oil to form a stable oil film [25]. The oil film on the rubbing surface played a part of the lubrication. MoS_2 nanosheets are supplied to the rubbing surfaces together with the oil phase. Layered structure of MoS_2 plays an important role in effective lubrication capability. Different from the single liquid lubricants, MoS_2 nanosheets can still be fixed at the rubbing surface under the extreme pressure underground. The lubricating decrease rate of JS-LUB is 96.5%, which is much higher than that of the commercial lubricants. Additionally, the drilling fluid density changed a little after adding JS-LUB but decreased obviously after the addition of KD-21C and KD-51. Foaming occurred after addition of KD-21C and KD-51 because of the existence of emulsifiers.

Table 1: Lubricity properties of lubricants in base drilling fluid.

Drilling fluid	Density ($g \cdot cm^{-3}$)	C_f	Lower rates of C_f (%)
Base drilling fluid	1.03	0.530	
Base drilling fluid + 0.5% base olefin	1.03	0.489	7.8
Base drilling fluid + 0.5% JS-LUB	1.03	0.019	96.5
Base drilling fluid + 0.5% KD-21C	1.01	0.058	88.4
Base drilling fluid + 0.5% KD-51	0.99	0.066	89.3

3.3. Compatibility Experiment of JS-LUB in the Field Drilling Fluid. Filed drilling fluid of Xu Zhuang block with the depth of 1200–1720 m was collected as a lubricant compatibility evaluation carrier in Xu49, which was similar to the drilling fluid in the testing well. Lithology in Sanduo layer is mainly including brown and dark brown mudstone shale strata, which is much easier transfer to mud. The drilling fluid mainly composed of PMHA polymer, bentonite, Na_2CO_3, Na-HPAN and mudstone hydrates from the stratum of Sanduo layer. Compatibility evaluation of the lubricants in the field drilling fluid was presented in Table 2.

As can be seen from Table 2, when KD-21C or KD-51 was added to the field drilling fluid, PV increases, and the rheological property changes obviously. That might be caused by the air bubbles formed by emulsifiers from lubricants. The rheological properties of drilling fluid were kept almost

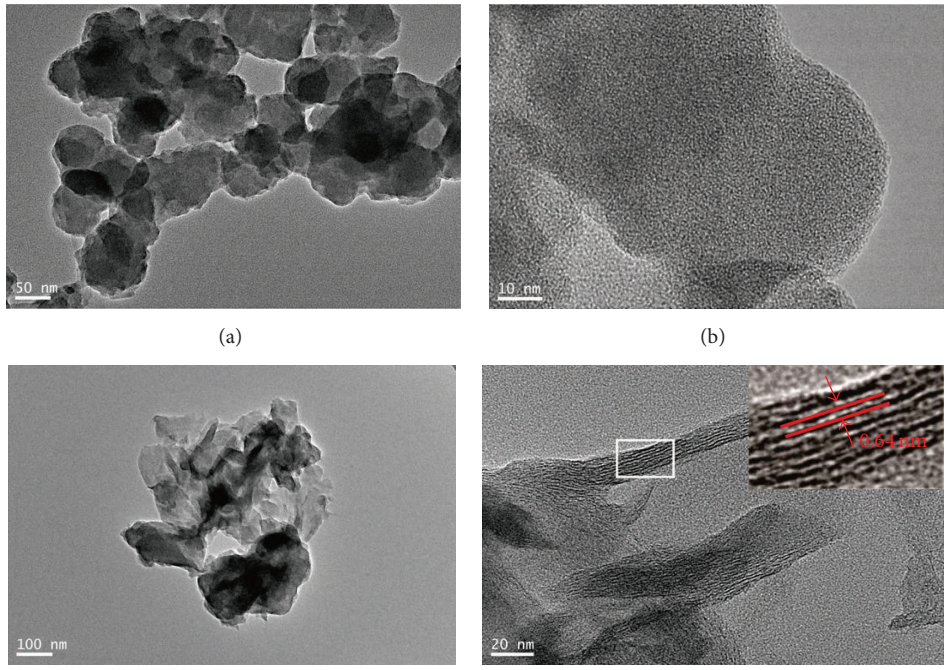

Figure 2: TEM and HRTEM photos of (a), (b) RM-MoS_2 and (c), (d) DDT-MoS_2.

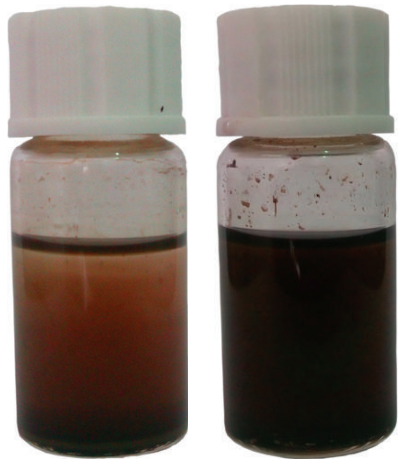

Figure 3: Dispersion state of MoS_2 nanosheets in base olefin after 24 h: (a) RM-MoS_2 and (b) DDT-MoS_2.

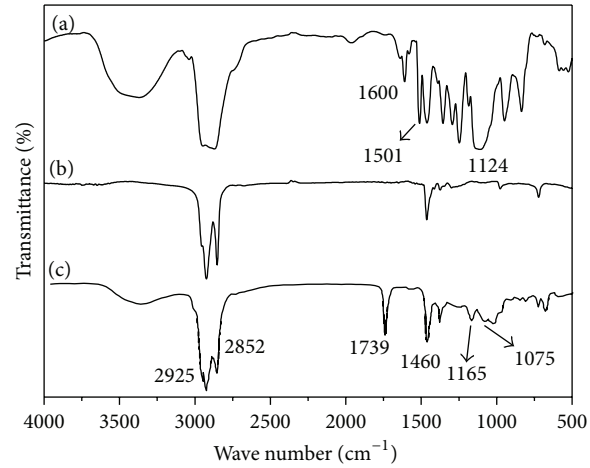

Figure 4: FTIR spectra of (a) JS-LUB, (b) DDT-MoS_2, and (c) RM-MoS_2.

constant with the addition of JS-LUB. Meanwhile, all of the lubricants exhibited the reducing of fluid loss with different degrees. This is because of a certain clogging effect on the tiny pores surface by oil film or droplets from the lubricants. Compared with KD-21C or KD-51, JS-LUB has no effect on the density of the drilling fluid and less effect on rheology variation, which would avoid complications due to drilling fluid properties changes caused by the lubricants.

3.4. Field Application. Xu50 was an exploration well, which was located in Shaobo town Yangzhou city, Jiangsu province. It was a spatial 3D directional well. The vertical depth was 2130 m, the kick-off point was 980 m, and the biggest hole angle was 40°. For comparison purposes, KD-21C and KD-51 were used in the neighbor wells named Xu47A and Xu-X48, respectively, with similar borehole curvature of Xu50 in the same oilfield block. JS-LUB was used in Xu50. The downhole stratum of Xu50 was composed by soft drilling fluid stone,

Table 2: The influence of lubricants on field drilling fluid behavior.

Drilling fluid	AV (mPa·s)	PV (mPa·s)	YP (Pa)	YP/PV	FL_{API} (mL)	Density ($g \cdot cm^{-3}$)
Field drilling fluid						
BR	20.5	14	6.5	0.46	5.6	1.12
AR	22	16	6	0.38	5.4	1.12
Field drilling fluid + 1% JS-LUB						
BR	21.5	15	6.5	0.43	4.8	1.12
AR	22.5	16	6.5	0.41	4.8	1.12
Field drilling fluid + 1% KD-21C						
BR	25	18	7	0.39	5.5	1.11
AR	30	20	10	0.5	5.3	1.11
Field drilling fluid + 1% KD-51						
BR	26	18	8	0.44	5.4	1.09
AR	31	21	10	0.48	5.2	1.08

Note: BR, before hot rolling; AR, after hot rolling. Hot rolling conditions: continuous rolling under 100°C for 16 hours.

which meant that it is necessary to improve ROP to avoid collapse, necking in building-up section.

In order to save costs in the region of Jiangsu oilfield, lubricants are used in a manner of gradually added type. Significant obstacle was captured when the deviation reached 29.6° with the well depth of 1542 m. 0.3 wt% of JS-LUB was added for the first time and then continuously added till 1.5 wt% until the well drilling was completed. After each addition of lubricants, the impact of drilling fluid with JS-LUB is shown in Table 3.

As can be seen from Table 3, after lubricant adding each time, no significant change of rheology was observed from the testing, and API filter loss declined slightly. Fluid density kept stability, which meant no bubbles producing after adding JS-LUB. The results showed that stable drilling performance without variation could be obtained in building-up section after JS-LUB adding. For the first time in 0.3% after adding lubricant, single sliding drilling rate did not change significantly. Continuing to add 0.4% lubricant, ROP increasing rate of single drill pipe increased 420%. In the depth of 1840 m, ROP increasing rate of single drill pipe increased 84% after adding 0.4% lubricant. The result means that the speed of single drill pipe increased significantly.

Figure 5 shows the ROP data collection with the well depth from Xu50 and Xu47A. Amount of 1.8-ton KD-21C, 1-ton KD51, and 0.5-ton base olefin was consumed in Xu47A. The total amount of JS-LUB used in Xu50 was 3 tons.

As can be seen from Figure 5, Xu50 and Xu47A have similar well depth and borehole curvature. There was no obscure ROP difference between the two wells while the borehole curvature was less than 30°. While the borehole curvature was over 30°, the frictional force between drilling tools and palisades increased substantially. ROP decreased while the borehole curvature was over 30°. Fortunately, ROP of Xu50 was much higher than that of Xu47A, which meant the lubricity of JS-LUB with the combination of MoS_2 nanosheets additive and liquid oil lubricant was more effective than KD-21C and KD-51.

Figure 6 shows the ROP data collection with the well depth from Xu50 and Xu-X48. Different from Xu47A, slide

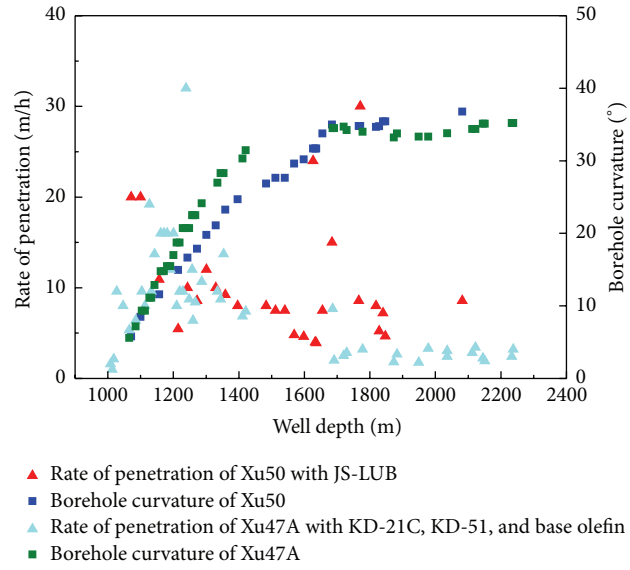

Figure 5: Rate of penetration of Xu50 and Xu47A.

drilling section of Xu-X48 was only before the well depth of 1500 m. Slide drilling tracks of Xu-X48 were similar with that of Xu50 while borehole curvature was over 30°. Smaller amount of lubricant was used in Xu-X48 due to the shallower slide drilling section. The total KD-51 depletion of Xu-X48 was 2.5 tons.

From Figure 6, ROP with JS-LUB in Xu50 was significantly higher than Xu-X48 with KD-51. While the drilling was completed, average drilling velocity and average ROP of Xu50 and the neighbor wells were collected and presented in Table 4.

As shown in Table 4, average ROP of Xu 50 was 10.03 m/h, which was 52.9% higher than that of Xu 47A with the same well depth and slide drilling tracks. In the case of slide drilling depth significantly greater than that of Xu X48, average ROP of Xu 50 was 139% higher than Xu X48. The average drilling velocity was about 20% higher than both neighbor wells,

Table 3: The impact of drilling fluid with JS-LUB.

Proportion of JS-LUB (%)	Well depth (m)	Borehole curvature (°)	FV (s)	PV (mPa·s)	YP (Pa)	YP/PV	FL_{API} (mL)	Density (g/cm^3)	ROP of single drill pipe (m/h)	Increasing rate of ROP (%)	Adding JS-LUB
0.3	1580	29.60	50	20	6	0.3	5.0	1.15	4.8	0	Before
	1607	30.19	48	20	5	0.25	4.8	1.15	4.61		After
0.4	1607	30.19	48	20	5	0.25	4.8	1.15	4.61	420	Before
	1630	32.00	47	19	6	0.32	4.8	1.15	24		After
0.4	1840	36.00	48	20	6	0.3	4.8	1.15	4.67	84	Before
	1848	36.00	47	19	7.5	0.39	4.6	1.15	8.57		After
0.4	2080	36.78	48	20	6	0.3	4.6	1.15	—	—	Before
	2100	36.78	48	20	7	0.35	4.6	1.15	—		After

Note: the proportion of JS-LUB was JS-LUB in total drilling fluid.

Table 4: Average rate of penetration of experimental well and contrasted wells.

Well number	Type of lubricant	The dosage of lubricant (T)	Average drilling velocity (m/h)	Average ROP* (m/h)	Increasing rate of ROP (%)
Xu 50	JS-LUB	3.0	15.04	10.03	
Xu 47A	KD-21C	1.8	12.22	6.56	52.9
	KD-51	1.0			
	Base olefin	0.5			
Xu X48	KD-51	2.5	12.57	4.20	139

*Average rate of penetration in downhole section with the borehole curvature over 30°.

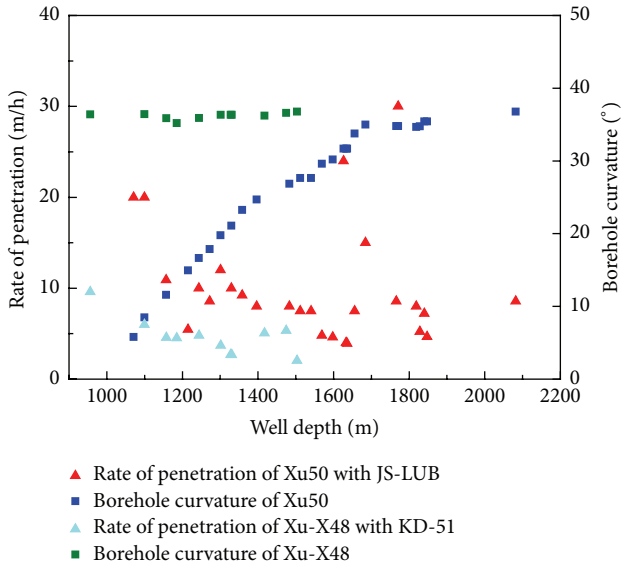

Figure 6: Rate of penetration of Xu50 and Xu-X48.

which demonstrated that the lubricity performance of MoS_2 nanosheets additive was more effective in building-up section of directional wells.

4. Conclusions

The MoS_2 nanosheets with particle size of about 100 nm were prepared in microemulsion. After high temperature annealing, dodecanethiol was used to modify the surface of the MoS_2 nanosheets. The modified MoS_2 nanosheets were then dispersed in liquid lubricant as an enhanced additive. The lubricant was used in water based drilling fluid system to increase the rate of penetration (ROP) in directional well. Field application results showed that ROP with the forth-putting of JS-LUB was 52.9% higher than that of the similar directional well with the traditional lubricants at least. The average drilling velocity was about 20% higher than the neighbor wells, which demonstrated that the lubricity performance of MoS_2 nanosheets was more effective in building-up section of directional wells.

Competing Interests

The authors declare that there are no competing interests regarding the publication of this paper.

Acknowledgments

This work was financially supported by State Key Laboratory of Heavy Oil Processing (SKLOP201602002) and the Fundamental Research Funds for the Central Universities (15CX05009A).

References

[1] H. Zhang, B. Hou, G. Yin et al., "The damage and deformation mechanism of soft mudstone in drilling engineer," *Advanced Materials Research*, vol. 524–527, pp. 1610–1614, 2012.

[2] S. H. Elrod and W. B. Nance, "Aqueous drilling fluid and lubricant composition," US Patent 4181617, 1980.

[3] D. Kania, R. Yunus, R. Omar, S. Abdul Rashid, and B. M. Jan, "A review of biolubricants in drilling fluids: recent research, performance, and applications," *Journal of Petroleum Science & Engineering*, vol. 135, pp. 177–184, 2015.

[4] F. M. T. Luna, J. B. Cavalcante, F. O. N. Silva, and C. L. Cavalcante Jr., "Studies on biodegradability of bio-based lubricants," *Tribology International*, vol. 92, pp. 301–306, 2015.

[5] L. Yang, L. Zhao, and G. Luo, "Study on the stability of emulsifying wax by turbidity ratio measurements," *Petroleum Processing and Petrochemicals*, vol. 42, no. 8, pp. 93–96, 2011.

[6] T. Xiang and R. A. M. Amin, "Water-based mud lubricant using fatty acid polyamine salts and fatty acid esters," US patent, patent number. 8413745, 2013.

[7] A. Navarro, W. R. Dannels, and AADE, "Maximizing drilling operationsby mitigating the adverse effects of friction through advanced drilling fluid technology," in *American Association of Drilling Engineers*, 2011.

[8] P. Keblinski, S. R. Phillpot, S. U. S. Choi, and J. A. Eastman, "Mechanisms of heat flow in suspensions of nano-sized particles (nanofluids)," *International Journal of Heat and Mass Transfer*, vol. 45, no. 4, pp. 855–863, 2002.

[9] W. Wang, K. Liu, and M. Jiao, "Thermal and non-Newtonian analysis on mixed liquid-solid lubrication," *Tribology International*, vol. 40, no. 7, pp. 1067–1074, 2007.

[10] S. M. S. Murshed, K. C. Leong, and C. Yang, "A combined model for the effective thermal conductivity of nanofluids," *Applied Thermal Engineering*, vol. 29, no. 11-12, pp. 2477–2483, 2009.

[11] B. Rahmati, A. A. D. Sarhan, and M. Sayuti, "Investigating the optimum molybdenum disulfide (MoS_2) nanolubrication parameters in CNC milling of AL6061-T6 alloy," *International Journal of Advanced Manufacturing Technology*, vol. 70, no. 5–8, pp. 1143–1155, 2014.

[12] S. Krishnan, Z. Abyat, and C. Chok, "Characterization of boron-based nanomaterial enhanced additive in water-based

drilling fluids: a study on lubricity, drag, ROP and fluid loss improvement," in *Proceedings of the SPE/IADC Middle East Drilling Technology Conference & Exhibition*, January 2016.

[13] D. B. Nimbalkar, H. H. Lo, P. V. R. K. Ramacharyulu, and S. C. Ke, "Improved photocatalytic activity of RGO/MoS_2 nanosheets decorated on TiO_2 nanoparticles," *RSC Advances*, vol. 6, no. 38, pp. 31661–31667, 2016.

[14] M. Zalaznik, S. Novak, M. Huskić, and M. Kalin, "Tribological behaviour of a PEEK polymer containing solid MoS_2 lubricants: tribological behaviour of a PEEK/MoS_2 polymer composite," *Lubrication Science*, vol. 28, no. 1, pp. 27–42, 2016.

[15] B. Chen, X. Li, X. Li et al., "Facile fabrication of hierarchical carbon fiber-MoS_2 ultrathin nanosheets and its tribological properties," *RSC Advances*, vol. 6, no. 65, pp. 60446–60453, 2016.

[16] D. Maharaj and B. Bhushan, "Effect of MoS_2 and WS_2 nanotubes on nanofriction and wear reduction in dry and liquid environments," *Tribology Letters*, vol. 49, no. 2, pp. 323–339, 2013.

[17] H. D. Huang, J. P. Tu, T. Z. Zou, L. L. Zhang, and D. N. He, "Friction and wear properties of IF-MoS_2 as additive in paraffin oil," *Tribology Letters*, vol. 20, no. 3-4, pp. 247–250, 2005.

[18] K. H. Hu, X. G. Hu, Y. F. Xu, F. Huang, and J. S. Liu, "The effect of morphology on the tribological properties of MoS_2 in liquid paraffin," *Tribology Letters*, vol. 40, no. 1, pp. 155–165, 2010.

[19] Z. Chen, H. Yan, T. Liu, S. Niu, and J. Ma, "Improved mechanical and tribological properties of bismaleimide composites by surface-functionalized reduced graphene oxide and MoS_2 coated with cyclotriphosphazene polymer," *RSC Advances*, vol. 5, no. 118, pp. 97883–97890, 2015.

[20] S.-D. Jiang, G. Tang, Z.-M. Bai, Y.-Y. Wang, Y. Hu, and L. Song, "Surface functionalization of MoS_2 with POSS for enhancing thermal, flame-retardant and mechanical properties in PVA composites," *RSC Advances*, vol. 4, no. 7, pp. 3253–3262, 2014.

[21] Z. Wu, D. Wang, Y. Wang, and A. Sun, "Preparation and tribological properties of MoS_2 nanosheets," *Advanced Engineering Materials*, vol. 12, no. 6, pp. 534–538, 2010.

[22] P. Pallavicini, A. Donà, A. Casu et al., "Triton X-100 for three-plasmon gold nanostars with two photothermally active NIR (near IR) and SWIR (short-wavelength IR) channels," *Chemical Communications*, vol. 49, no. 57, pp. 6265–6267, 2013.

[23] R. Brudler, R. Rammelsberg, T. T. Woo, E. D. Getzoff, and K. Gerwert, "Structure of the i1 early intermediate of photoactive yellow protein by FTIR spectroscopy," *Nature Structural Biology*, vol. 8, no. 3, pp. 265–270, 2001.

[24] E. Gat, M. A. El Khakani, M. Chaker et al., "A study of the effect of composition on the microstructural evolution of a-SixC1-x: H PECVD films: IR absorption and XPS characterizations," *Journal of Materials Research*, vol. 7, no. 9, pp. 2478–2487, 1992.

[25] F. Song, "A clean lubricant for drilling fluid and preparation method," CN patent, patent number. 20111061229, 2012.